J Mol Model (2013) 19:1667–1675
DOI 10.1007/s00894-012-1733-4

ORIGINAL PAPER

Silicon–doping in carbon nanotubes: formation energies, electronic structures, and chemical reactivity

Ruixin Bian · Jingxiang Zhao · Honggang Fu

Received: 7 November 2012 / Accepted: 13 December 2012 / Published online: 5 January 2013

Abstract By carrying out density functional theory (DFT) calculations, we have studied the effects of silicon (Si)-doping on the geometrical and electronic properties, as well as the chemical reactivity of carbon nanotubes (CNTs). It is found that the formation energies of these nanotubes increase with increasing tube diameters, indicating that the embedding of Si into narrower CNTs is more energetically favorable. For the given diameters, Si-doping in a (*n*, 0) CNT is slightly easier than that of in (*n*, *n*) CNT. Moreover, the doped CNTs with two Si atoms are easier to obtain than those with one Si atom. Due to the introduction of impurity states after Si-doping, the electronic properties of CNTs have been changed in different ways: upon Si-doping into zigzag CNTs, the band gap of nanotube is decreased, while the opening of band gap in armchair CNTs is found. To evaluate the chemical reactivity of Si-doped CNTs, the adsorption of NH_3 and H_2O on this kind of material is explored. The results show that N–H bond of NH_3 and O–H bond of H_2O can be easily split on the surface of doped CNTs. Of particular interest, the novel reactivity makes it feasible to use Si-doped CNT as a new type of splitter for NH_3 and H_2O bond, which is very important in chemical and biological processes. Future experimental studies are greatly desired to probe such interesting processes.

Keywords Chemical reactivity · DFT · Si-doped CNT

Introduction

Inclusion of non-carbon atoms into hexagonal of carbon nanotubes (CNTs) is an effective way to change or tailor their electronic and transport properties, which can be used for developing novel materials [1–4], such as enhanced filed emission devices, *n*- or *p*-type semiconductors, and full cell electrodes. Moreover, the chemical reactivity of CNTs can be greatly enhanced due to the doping, rendering them to have unique applications in gas detecting, support for catalytic particles, and protein immobilization. Hence, the doping of non-carbon atoms into CNTs has become a hot topic recently. Currently, the most common dopants of CNTs are boron (B) and nitrogen (N) atoms [5–8], which are the neighbors of carbon (C) atoms in the periodic table. Interestingly, B- or N-doping of CNTs can not only modify electronic structures of CNTs, but also endow CNTs with some new properties [9–17]. Nitrogen, for example, acts as an electron donor in a CNT since it has five valence electrons, causing a shift in the Fermi level to the valence bands. This makes all N-doped CNTs metallic in nature, regardless of their geometries [10]. Moreover, Zheng et al. have evaluated the effects of the doping of N atoms on the electronic and field emission properties of CNTs through first-principles calculations [11]. Zhou and Liu have independently suggested that B- and N-doped CNTs exhibit high reactivity toward NH_3 [12], NO_2 [12], and HCHO [14]. Additionally, Cho and co-workers have shown that the dissociation barriers of O_2 and H_2 on CNTs are greatly reduced due to the N-doping [16, 17]. In particular, facile

Electronic supplementary material The online version of this article (doi:10.1007/s00894-012-1733-4) contains supplementary material, which is available to authorized users.

J. Zhao · H. Fu (✉)
Key Laboratory of Functional Inorganic Material Chemistry, Ministry of Education of the People's Republic of China, Heilongjiang University, 150080 Harbin, People's Republic of China
e-mail: fuhg@vip.sina.cn

R. Bian · J. Zhao (✉)
College of Chemistry and Chemical Engineering, Harbin Normal University, Harbin 150025, People's Republic of China
e-mail: xjz_hmily@yahoo.com.cn

oxygen reduction reaction (ORR) has been observed experimentally in metal-free N-doped nanotubes very recently [18, 19].

Silicon (Si) is another electron donor that can be incorporated into the hexagonal lattice of single-walled CNTs. But fundamentally different from N, the valence electrons of Si atom are in the third shell. Theoretically, Si-doped CNTs have been for the first time proposed in 2001 by Baierle et al. [20], in which an empty level is induced above the top of the valence band. Furthermore, Avramov and Galano have independently investigated the stability and electronic properties of Si substituted CNTs [21, 22]. In addition, Zhang reported that the reactivity of CNTs is significantly enhanced because of the Si-doping, rendering Si-doped CNT a good candidate as a gas sensor or drug delivery device [23, 24]. Because the Si atom is larger than C atom and increases the disorder within hexagonal carbon framework, very recently, Terrones et al. have firstly synthesized the Si-doped CNT by using methoxytrimethylsilane as a precursor [25]. The synthesis of Si-doped CNTs will motivate more theoretical and experimental studies to explore their properties and applications. We note that although the above few studies have reported the electronic properties and reactivity of Si-doped CNTs [20–24, 26–31], there are still some unclear issues to be addressed: 1) how do the tube diameters and helicities of CNTs affect the stability of Si-doped CNTs? 2) How are the stabilities of doped CNTs with two Si atoms? 3) Since Si-doped CNTs might possess higher chemical reactivity toward adsorbates than pure CNTs, can they cleave some chemical bonds of small molecules, such as N–H or O–H bond (which is very important in chemical and biological processes)? In this paper, by performing the extensive density functional theory (DFT) calculations, we have answered the above questions point by point. The present work might be useful not only to deeply understand the experimental results of Si-doped CNTs, but also to further widen their application areas.

Computational methods

All-electron density functional theory (DFT) computations were carried out by employing the generalized gradient approximation (GGA) with the Perdew-Burke-Ernzerhof (PBE) [32] functional and the double numerical plus polarization basis set, which was implemented in the DMol3 package [33, 34]. Self-consistent field calculations were conducted with convergence criteria of 10^{-6} a.u. for the total energy. All systems were fully relaxed without any symmetry constraint. Along the 1D Brillouin zone, two k points were used for geometry optimizations and 21 k points for calculating the energies and electronic properties [35].

The curvature effect was discussed by considering a series of zigzag single-walled CNTs from (8, 0) tube (6.26 Å in diameter) to (13, 0) tube (10.18 Å in diameter). Moreover, a series of armchair nanotubes from (4, 4) tube (5.42 Å in diameter) to (8, 8) tube (10.85 Å in diameter) were adopted to discuss the helicity effects. Each nanotube was placed in a tetragonal supercell with sufficiently large lattice lengths perpendicular to the tube axes, i.e., 30 Å for these studied nanotubes. Along the tube axis, the supercell length was chosen to be 12.68 Å for zigzag tubes (three unit cells) and 14.76 Å for armchair tubes (six unit cells). With such large supercell dimensions, the interaction between Si-doped CNTs and their 1-D periodic images can be avoided.

The formation energy for Si-doping into the CNT was defined as: $E_F = (E_{t1}-E_{t2}) - m \times (E_1-E_2)$, where E_{t1} is the total energy of CNTs with substitutional doping, E_{t2} is the total energy of pristine CNTs, E_1 is the energy of single free doping atom, E_2 is the energy of single free carbon atom, and m is the number of doping atoms. The adsorption energy of NH_3 molecule on the Si-doped CNT was evaluated as: $E_{ads} = E_{total}$ (Si-doped CNTs/NH_3) – E_{total} (Si-doped CNTs) – E_{total} (NH_3), where E_{total} stands for the total energy of the studied systems. A negative E_{ads} corresponds to a stable structure. Furthermore, we used the linear/quadratic synchronous transit (LST/QST) [36, 37] method to obtain the given energy barriers. In essence, the synchronous transit methods interpolate a reaction pathway to find a transition state starting with the initial and final structures of the reaction system. The linear synchronous transit (LST) method performs a single interpolation to a maximum energy. The quadratic synchronous transit (QST) method alternates searches for an energy maximum with constrained minimizations in order to refine the transition state to a high degree. The complete LST/QST method begins by performing an LST/optimization calculation. The TS approximation obtained in that way is used to perform the QST maximization. From that point, another conjugate gradient minimization is performed. The cycle is repeated until a stationary point is located or the number of allowed QST steps is exhausted.

Results and discussion

Local structures of Si-doped CNTs

First, taking (10, 0) and (5, 5) CNTs as examples, we study the effects of Si-doping on the geometrical structures of CNTs. After fully structural optimizations, Si-doping causes significantly large distortion in CNTs (Fig. 1): i.e., the nonequivalent Si–C bond lengths in doped (10, 0) CNT are 1.744 (axial) and 1.817 Å (diagonal), which are significantly larger than the C–C sp^2 bonds (1.420 Å) of pristine

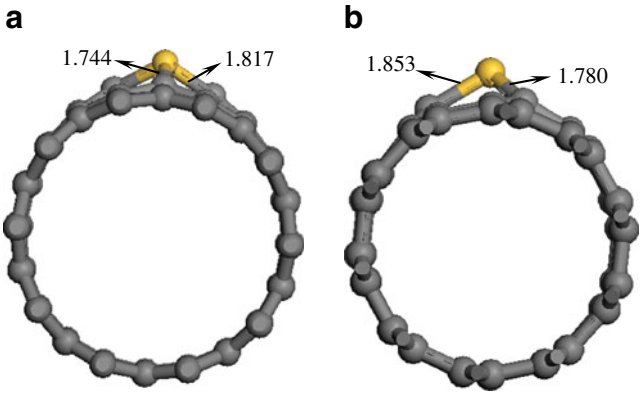

Fig. 1 The optimized structures of Si-doped (**a**) (10, 0) and (**b**) (5, 5) CNTs. The bond distances are in angstroms

CNT. Moreover, Si atom preserves its sp^3 character, and bonds with tetrahedral-like configurations, with the average C–Si–C bond angles of 100°. The increase in the bond lengths combined with the difference in bond angles forces the Si atom to protrude outwardly from the nanotube surface. Meanwhile, the positions of the nearest C atoms of Si atom are out of the nanotube surface to different degrees. As a result, the nanotube diameter at the Si site is increased from 7.830 Å (pure CNT) to 9.075 Å (Si-doped CNT). These changes in the structures of CNT originate from the corrugation induced by the presence of the Si atom. The calculated energy of forming Si-doped (10, 0) CNT is about 7.405 eV.

As shown in Fig. 1b, the structural changes of in (5, 5) CNT due to Si-doping are very similar to those of (10, 0) nanotube: (1) the Si–C bond lengths are 1.780 Å for the diagonal and 1.853 Å for the tangential bonds, while the angles are also close to 100°; (2) Si atom protrudes outwardly from the nanotube wall, and the tube diameter at the defect site is 7.843 Å, which is much larger than that of the pristine nanotube (6.780 Å). Moreover, the calculated formation energy of Si-doped (5, 5) CNT is 7.142 eV. In addition, we extended our calculations to other (n, 0) (n= 8–13) and (n, n) (n=5–8) CNTs. The results show that the changes in structures of CNTs are very similar to the cases of (10, 0) and (5, 5) CNTs.

In the literature, we note that the formation energies of the doped CNTs by non-carbon atoms are significantly dependent on the tube diameter and helicity [11, 25]. For example, Zheng et al. reported that the curve of formation energies of N-doped (n, 0) CNTs exhibits the feature of periodicity, and such periodicity is characterized by the lower formation energies of doped tubes with n as a multiple of 3 as compared to their neighboring tubes [11]. On the contrary, the incorporation of the phosphorus (P) atom in the hexagonal carbon lattice is energetically favored in narrower nanotubes that exhibit higher diameters of curvature [25, 38]. In terms of the two studies, a question arises: how do the diameters and helicities of CNTs affect the formation energy of Si-doping, which is similar to N-doping, or P-doping? In Fig. 2a, we plot the calculated formation energy (E_F) as a function of the diameter and helicity of CNTs. It can be obviously seen that (1) the energies of forming Si-doped CNTs increase with increasing tube diameters. The smallest diameter (8, 0) CNT has the lowest formation energy (4.639 eV). In other words, Si-doping in narrower diameter CNTs is energetically preferable, which is similar to the case for P-doped CNTs [25, 39]. This is expected, because the curved nanotube structure helps to reduce the strain needed to accommodate the silicon impurity. (2) For a given diameter, the forming energies of armchair CNTs are always slightly larger than those of zigzag CNTs, suggesting that Si-doped zigzag CNTs might be easier to obtain in experiment.

The next question is what will happen if two Si atoms are introduced into CNTs. The (10, 0) is chose as a typical tube to investigate this question. We consider two kinds of initial doped configurations, i.e., the two doped Si atoms might be very near to or far from each other. For the former case, six configurations (labeled as Si1, Si2, Si3, Si4, Si5, and Si6, respectively, Fig. 3a–f) are considered, in which two Si atoms lie in the same hexagon. For the latter case, two Si

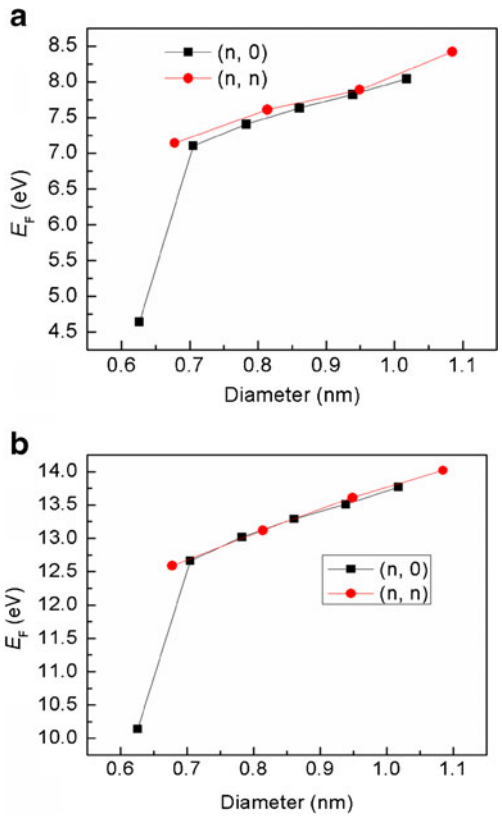

Fig. 2 Variation of formation energies of Si-doped CNTs as a functional of tube diameters: **a** the doped CNTs with one Si atom and (**b**) the doped CNTs with two Si atoms

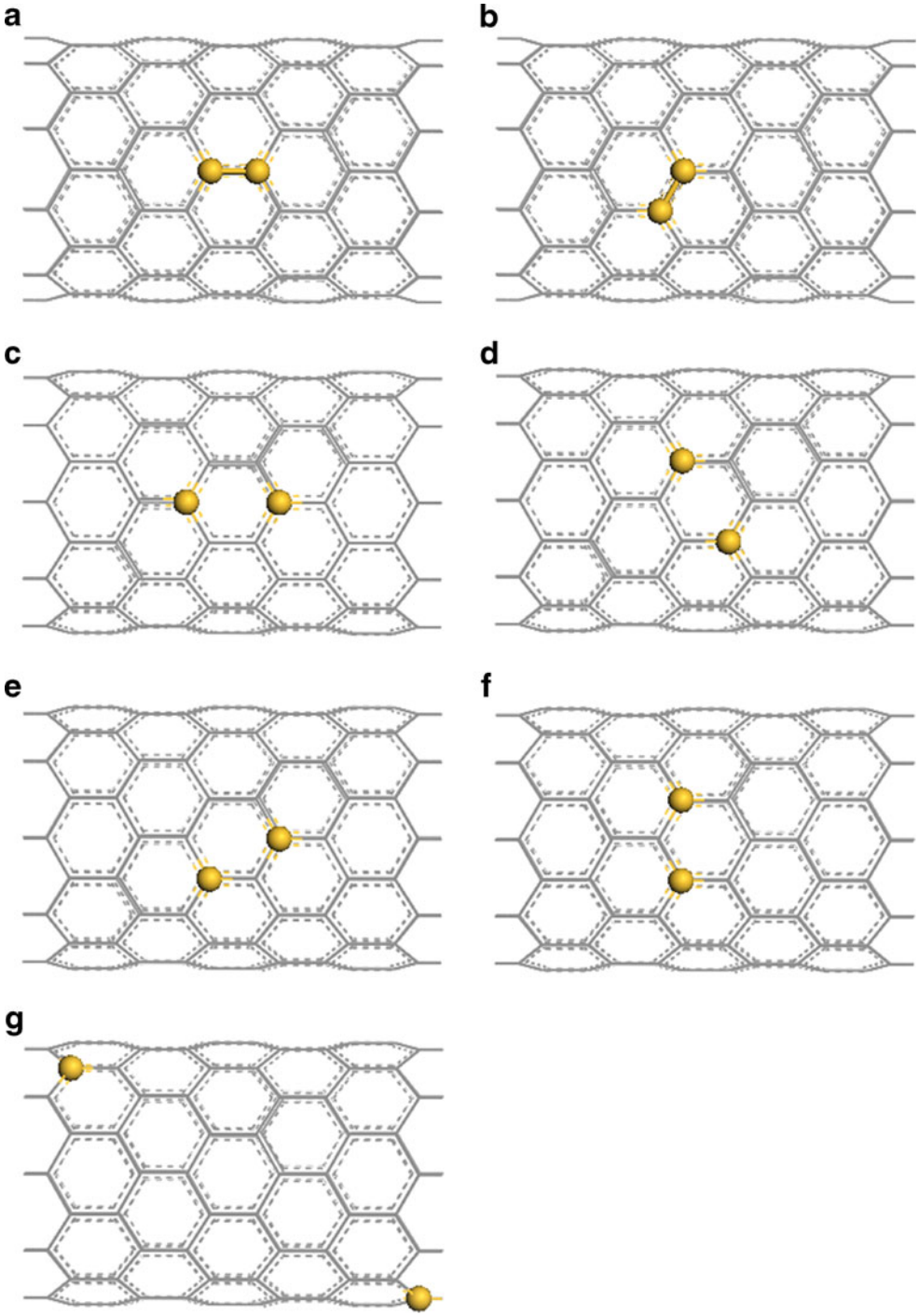

Fig. 3 Schematic descriptions of the configurations for (10, 0) tubes containing two substitutional silicon atoms, which are denoted as Si1 (**a**) – Si7 (**g**). The substitutional silicon atoms are denoted by yellow balls

atoms are far apart (labeled as Si7, Fig. 3g). The calculated total energies and the Si–Si bond lengths of these doped (10, 0) CNTs with two Si atoms are listed in Table 1. It is clear that the Si6 configuration has the lowest energy, indicating that it is the most energetically favored among these doped (10, 0) CNTs. Moreover, the calculated formation energy for the Si6 configuration is 13.022 eV, which is smaller than double of the doped (10, 0) CNT by one Si atom (7.405 eV×2=14.810 eV). Therefore, the double substituted CNT are easier to form than that of with one Si atom. This is similar to BN-co-doped CNTs, in which the total energy with an adjacent B/N atom pair is lower than those with separately doped B and atoms at different position [39, 40]. Moreover, for the double substituted (10, 0) CNT (Fig. 4a), the two Si atoms are pulled outwardly from the tube surface and the Si–Si bond length is 3.097 Å. For the double doped (5, 5) CNT, the most stable configuration is shown in Fig. 4b, in which the two Si atoms are separated by two C

Table 1 Electronic energies (a.u.) and Si-Si bond lengths (Å) for double substituted (10, 0) CNTs

	Si1	Si2	Si3	Si4	Si5	Si6	Si7
Energy	-5072.008	-5072.027	-5072.029	-5072.029	-5072.017	-5072.030	-5072.003
d(Si-Si)	2.123	2.252	2.755	3.353	2.780	3.097	10.276

atoms. The formation energy is 12.594 eV with the Si–Si bond length of 3.520 Å. We also calculate the effects of the diameters and helicities of CNTs on the formation energies of double substituted CNTs. Similar to the case of single doped CNTs, the incorporation of two Si atoms in the narrower CNTs is energetically favorable (Fig. 2b).

The effects of Si-doping on the electronic properties of CNTs

One purpose of introducing Si atoms into CNTs is to modify their electronic properties. In this section, we study the effects of Si-doping on the electronic properties of CNTs. The band structures of perfect and doped (10, 0) CNTs are investigated as shown in Fig. 5. For the perfect (10, 0) CNT, the band gap between the bottom of the conduction band and the top of the valence band at the Γ point is about 0.625 eV (Fig. 5a). When one Si atom is doped into the (10, 0) CNT, an empty level at the bottom of the conduction band is induced into the band structures (Fig. 5b), decreasing its band gap to 0.409 eV. For double substituted (10, 0) CNT, due to the introduction of two new states, the band gap of (10, 0) CNT is further decreased to 0.376 eV (Fig. 5c). Interestingly, when the metallic (5, 5) CNT is doped with one or two Si atoms, its band gap is increased to 0.163 (one Si-doping, Fig. 5d) and 0.218 eV (two Si-doping Fig. 5e). This implies that Si-doping into metallic CNTs can open a tunable band gap.

It is well known that Si atom might work as a donor when incorporated into CNTs. Therefore, the highest occupied level (highest occupied molecular orbital, HOMO) for the doped CNTs are mainly contributed by the excess electrons of Si atoms. This can be testified by the distribution of HOMO of doped CNTs (Fig. 6): most states of the HOMOs are localized around the Si atoms. Moreover, the population

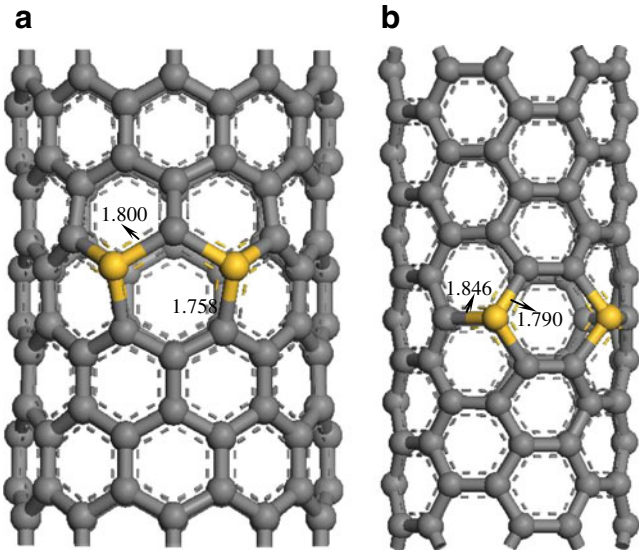

Fig. 4 The most stable configurations of doped (**a**) (10, 0) and (**b**) (5, 5) CNTs with two Si atoms. The bond distances are in angstroms

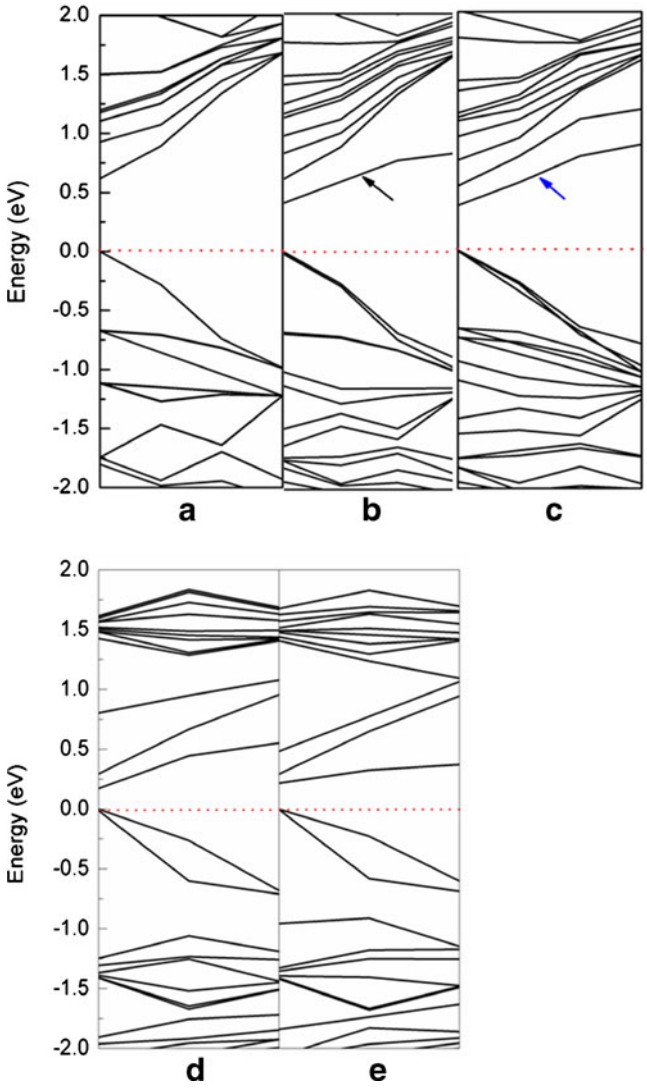

Fig. 5 The band structures for (**a**) a pure (10, 0) CNT, **b** doped (10, 0) CNT with one Si atom, **c** doped (10, 0) CNT with two Si atoms, **d** doped (5, 5) CNT with one Si atom, and (**e**) doped (5, 5) CNT with two Si atoms. The Fermi level is set as zero

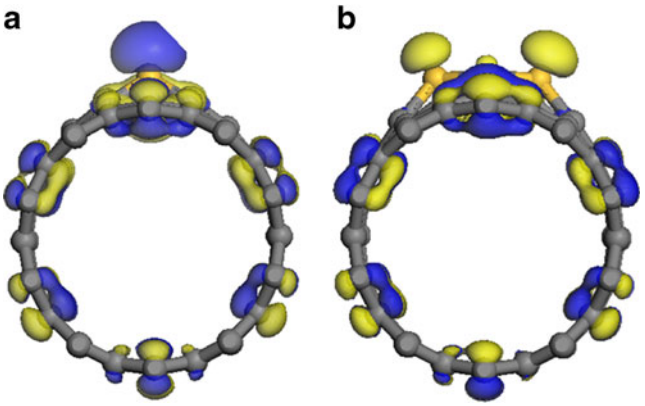

Fig. 6 Qualitative descriptions of the highest occupied levels of a (10, 0) tube with (**a**) one and (**b**) two substitutional Si atoms

analysis suggests that the charges of the Si atoms of doped CNT are much larger than those of the carbon atoms around Si atoms. For example, the charges of Si atoms in single and double doped (10, 0) CNTs are 0.824 and 0.909 e. Thus, the Si atom in Si-doped CNTs might be the reactivity center toward foreign adsorbates, which will be proven in the following section.

Chemical reactivity of Si-doped CNT

Recently, Zhang et al. have studied the reactivity of Si-doped CNTs toward small gaseous molecules in the atmosphere [23, 24]. They have found that the reactivity of CNT can be significantly enhanced due to the Si-doping, rendering Si-doped CNTs to have potential applications in gas sensing [23] and drug delivery [24]. This gives us an inspiration: since Si-doped CNTs possess higher chemical

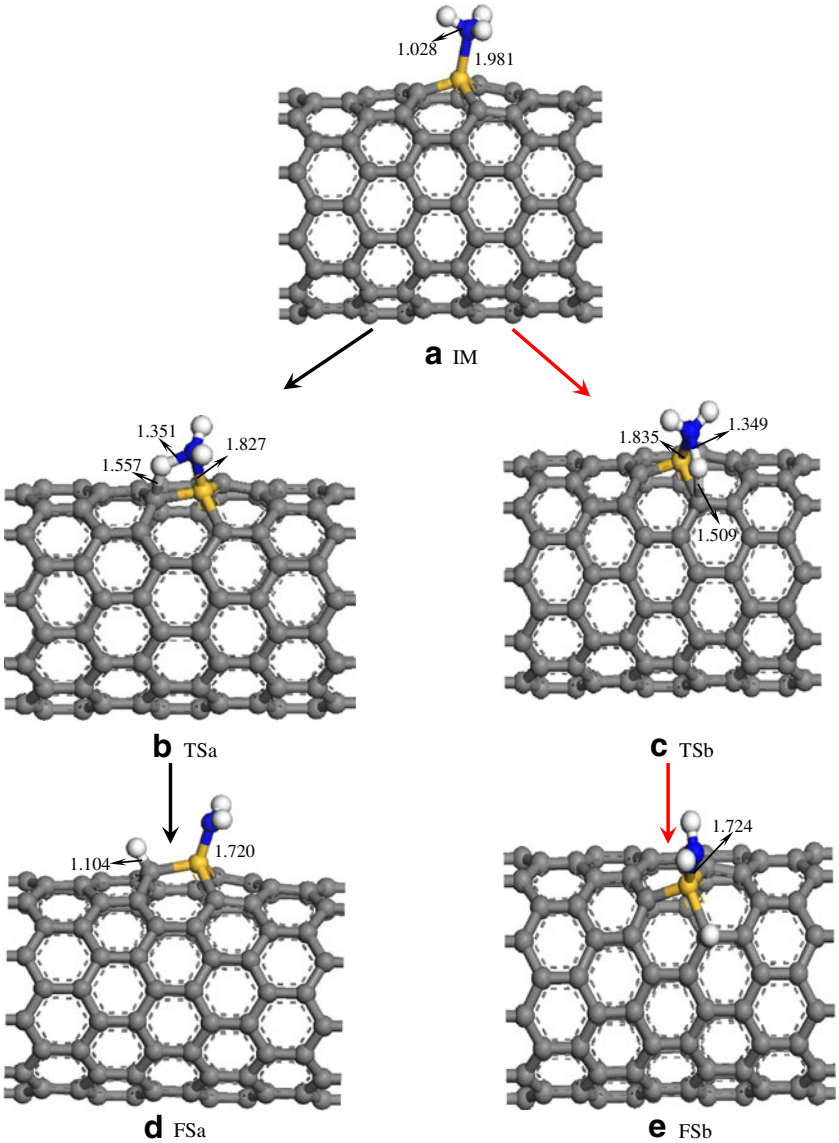

Fig. 7 The optimized structures of the (**a**) initial state (denoted as IS), **b** and (**c**) transition states (denoted as TSa and TSb), **d** and (**e**) final states (denoted as FSa and FSb) of the N-H bond cleavage of NH_3 on Si-doped (10, 0) CNT. The bond distances are in angstroms

reactivity than pure CNTs, can they further catalyze the adsorbed molecules? In fact, a stronger binding strength between the adsorbates and the Si-doped CNT may promote associated product formation. This is of vital importance to design novel ***metal-free*** catalysts. Considering NH_3 and H_2O are two important compounds in nature, we have evaluated the chemical reactivity of Si-doped CNTs by studying the NH_3 and H_2O adsorption on Si-doped CNTs.

In detail, for NH_3 and H_2O adsorption on Si-doped (10, 0) CNTs, we considered two kinds of initial adsorption sites, i.e., (1) Si site and (2) its neighboring C site. After full structural optimization for each initial configuration, we find that NH_3 and H_2O adsorption on the C sites around Si site are collapsed to Si site, which is the only energetically stable type. As shown in Fig. 7a, the distance between NH_3 and doped (10, 0) CNT with one Si atom is 1.981 Å, which is longer than that of H_2O adsorption (2.003 Å, Fig. 8a). Correspondingly, the adsorption energy of NH_3 on Si-doped CNT (−1.219 eV) is larger than that of H_2O (−0.570 eV). Since NH_3 and H_2O can be molecularly adsorbed on Si-doped CNTs with high exothermicity (−1.219 eV for NH_3 and −0.570 eV for H_2O), can the N–H of the adsorbed NH_3 and O–H bonds of the adsorbed H_2O be split on Si-doped CNT? Hence, we compute the minimum-energy path (MEP) for the split of N–H bond of NH_3 and O–H bond of H_2O on (10, 0) Si-doped CNT using the nudged elastic band (NEB) method [36, 37]. We choose the molecular adsorption of NH_3 and H_2O on the Si-doped

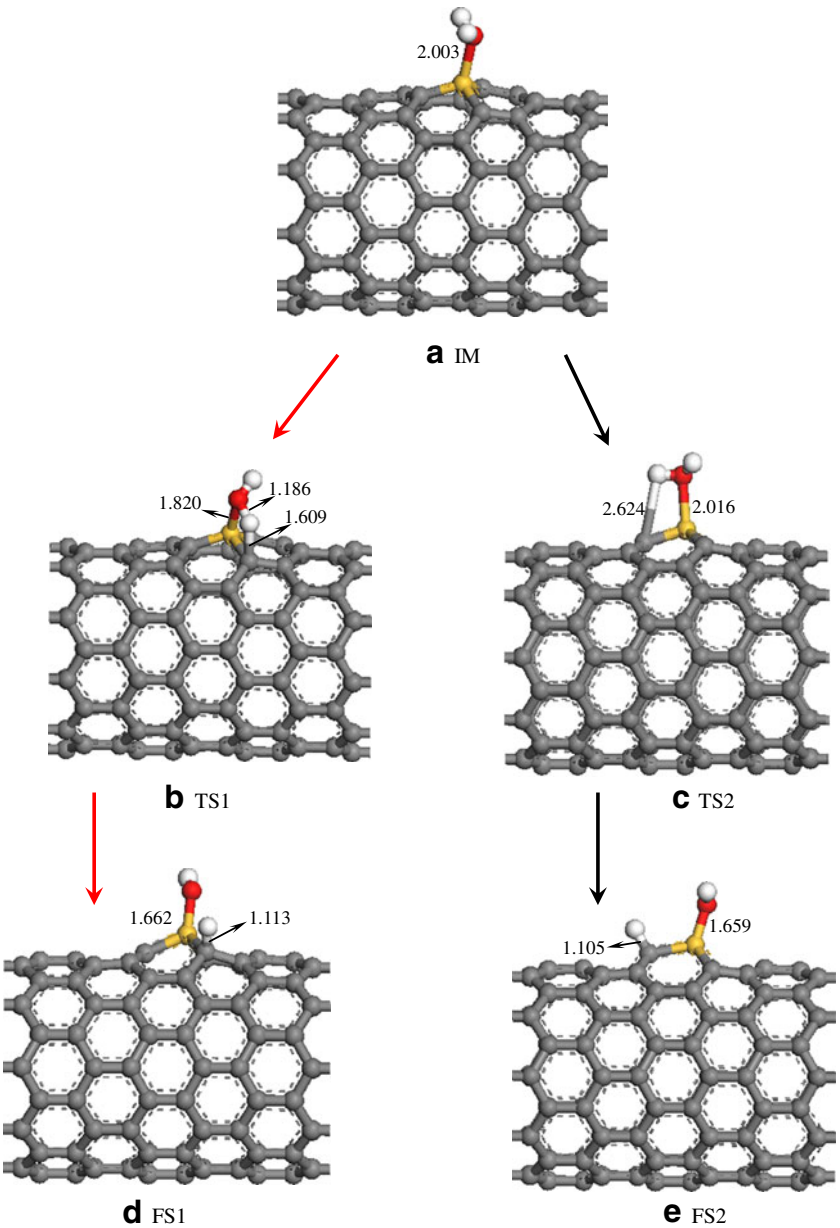

Fig. 8 The optimized structures of the (**a**) initial state (denoted as IS), **b** and (**c**) transition states (denoted as TS1 and TS2), **d** and (**e**) final states (denoted as FS1 and FS2) the O-H bond cleavage of H_2O on Si-doped (10, 0) CNT. The bond distances are in angstroms

(10, 0) CNT as the initial states (denoted as IS, Figs. 7a and 8a) and the split configuration as the final states (denoted as FS, Figs. 7b, c, 8b, and c). To achieve sufficient accuracy for the MEP, 20 image structures are inserted between the initial and final state.

Figure 9 lists the computed MEP for the cleavage of the N–H and O–H bonds on (10, 0) Si-doped CNT. The results suggest that: (1) in the doped CNT with one Si-atom, the H atom of the adsorbed NH_3 on Si site prefers to be transferred to the diagonally neighboring C atom (Fig. 7c) with the intrinsic barrier of 1.052 eV. (2) For the adsorbed H_2O on the Si site, the O–H bond can also be further split, in which the H atom is transferred to the axial C site nearest (Fig. 8b). Moreover, the intrinsic H-transfer barrier of H_2O cleavage (0.072 eV) is much smaller than that of NH_3 (1.052 eV). This seems to correlate with the binding strength of O–H and N–H bonds. (3) The H_2O cleavage has an extremely high reaction energy

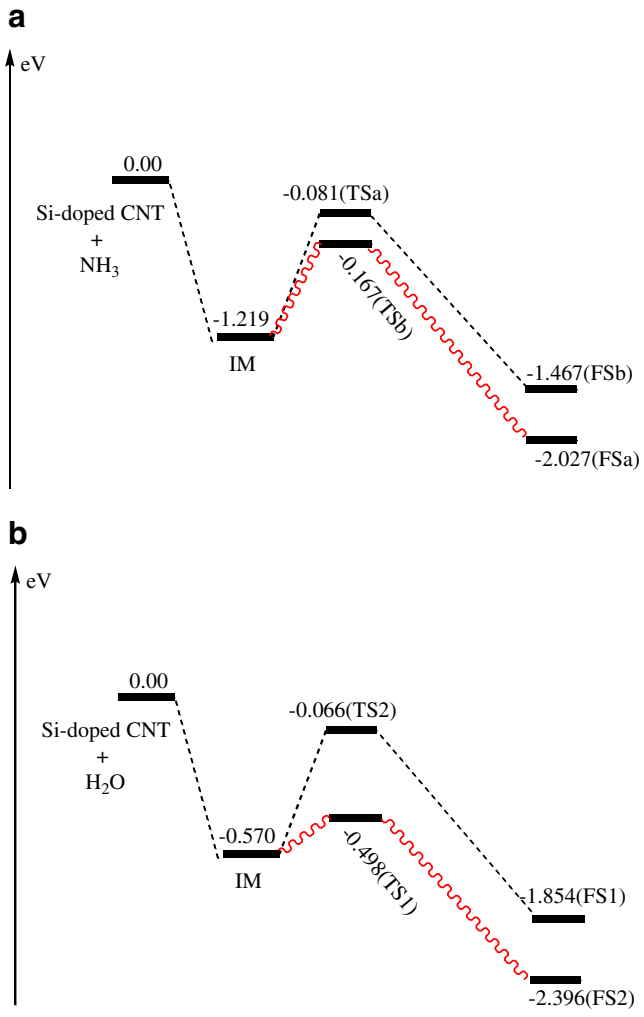

Fig. 9 Schematic energy profile corresponding to local configuratons shown in Figs. 7 and 8 along the minimum-energy pathway for (**a**) N–H and (**b**) O–H cleavage process on Si-doped (10, 0) CNT. All energies are given with respect to the reference energy

of −2.396 eV, which is slightly larger than that of NH_3 cleavage (−2.027 eV). The difference in reaction energy between NH_3 and H_2O on Si-doped CNTs is because the binding energy of the Si–O bond (798 $kJmol^{-1}$) is larger than that of the Si–N bond (439 $kJmol^{-1}$) [41]. (4) Because the energies released by molecular adsorptions of NH_3 (−1.219 eV) and H_2O (−0.570 eV) on Si-doped CNT are larger than their required H-transfer barrier (1.052 eV for NH_3 and 0.072 eV for H_2O), we expect that the N–H bond of NH_3 and O–H bond of H_2O can be easily split on Si-doped CNT. It should be pointed out that we also study the chemical reactivity of the double Si-doped CNT. As shown in Fig. S1 of **Supporting information**, it is found that the N–H bond of NH_3 can also easily occur and the process is similar to the case of doped CNT with one Si atom. The involved intermediates, transition states, and products are listed in Fig. S2.

The two unknown reactions Si-doped CNTs + NH_3/H_2O should have potential interest in the N–H and O–H splitting chemistry, which is very important in chemical and biological processes. In particular, the N–H activation has become the current hot topic. In addition to the potential use in initiating new valuable catalytic reactions, the effective activation of the N–H bond under mild conditions can help synthesize various amino compounds, which are building blocks for myrid substances ranging from proteins to pharmaceuticals. Due to the strong N–H bond, successful examples of NH_3-splitting are still rare in laboratory [42–48]. Of particular interest, the metal-free N–H activation system has been limited to the acyclic and cyclic (alkyl)(amino) carbenes [48]. Compared with carbenes-based metal-free NH_3 splitter, our work provides an alternative promising ***metal-free*** system for NH_3-splitting, which has high-surface area, good electrical and mechanical properties, and superb thermal stability.

Conclusions

Si-doping in a series of single-walled CNTs has been investigated through DFT theory. The results indicate that the Si-doping induces structural deformation in CNTs and changes the local curvature at doping sites. The tube diameter, helicity, and the number of Si atoms determine the doping formation energies: (i) Si-doping easily forms in small diameter CNTs; (ii) the doped (n, 0) CNTs are preferred energetically over (n, n) CNTs; (iii) the doping of two Si atoms into CNTs is easier than that of a single Si atom. Moreover, Si-doping induces impurity states into the band structures of CNTs, decreasing the band gap of (n, 0) CNTs and opening the band gap of (n, n) CNTs. In addition, the reactivity of Si-doped CNTs is evaluated by NH_3 and H_2O adsorption. It is found that the N–H bond of NH_3 and O–H bond of H_2O can be easily split on the Si-doped CNTs and a two-step mechanism is involved in this process: (1) molecular adsorption of NH_3 and H_2O on the Si

site in Si-doped CNTs followed by (2) the H-transfer to the neighboring C site. The present results might be helpful not only to deeply understand the experimental results, but also to provide a useful guidance to develop novel CNTs-based ***metal-free*** catalysts.

Acknowledgments We gratefully acknowledge the support of this research by the Key Program Projects of the National Natural Science Foundation of China (No 21031001, 20971040, 21001042, 21203048), the Cultivation Fund of the Key Scientific and Technical Innovation Project, Ministry of Education of China (No 708029), Specialized Research Fund for the Doctoral Program of Higher Education of China (20112301110002), the University Key Teacher Foundation of Heilongjiang Provincial Education Department (NO: 1252G030), the China Postdoctoral Science Foundation (20110491119), and Heilongjiang Postdoctoral Science Foundation (LBH-Z10049). The authors would like to show great gratitude to the reviewers for raising invaluable comments and suggestions.

References

1. Treacy MJ, Ebessen TW, Gibson JM (1996) Nature 381:678–680
2. Tans SJ, Devoret MH, Dai H, Tess A, Smalley RE, Gerligs LJ, Dekker C (1997) Nature 386:474–477
3. Tans SJ, Verschueren ARM, Dekker C (1998) Nature 393:49–52
4. Terrones M, Souza Filho AG, Rao AM (2008) Doped carbon nanotubes: synthesis, characterization and applications. In: Jorio A, Dresselhaus MS, Dresselhaus G, (eds) Carbon nanotubes: advanced topics in the synthesis, structure, properties and applications. Springer, Berlin, 531:566
5. Gai PL, Stephan O, McGuire K, Rao AM, Dresselhaus MS, Dresselhaus G, Colliex C (2004) J Mater Chem 14:669–675
6. Villap OF, Zamudio A, Elias AL, Son H, Barros EB, Chow SG, Kim YA, Muramatsu H, Hayashi T, Kong J, Terrones H, Dresselhaus G, Endo M, Terrones M, Dresselhaus MS (2006) Chem Phys Lett 424:345–352
7. McGuire K, Gothard N, Gai PL, Dresselhaus MS, Sumanasekera G, Rao AM (2005) Carbon 43:219–227
8. Sumpter BG, Meunier V, Romo-Herrera JM, Cruz-Silva E, Cullen DA, Terrones H, Smith DJ, Terrones M (2007) ACS Nano 1:369–375
9. Ayala P, Rubio A, Pichler T (2010) Rev Mod Phys 82:1843–1885
10. Terrones M, Jorio A, Endo M, Rao AM, Kim YA, Hayashi T, Terrones H, Charlier JC, Dresselhaus G, Dresselhaus MS (2004) Mater Today 7:30–45
11. Yu SS, Wen QB, Zheng WT, Jiang Q (2007) Nanotechnology 18:165702
12. Bai L, Zhou Z (2007) Carbon 45:2105–2110
13. Li Y, Zhou Z, Shen P, Chen Z (2009) ACS Nano 3:1952–1958
14. Wang RX, Zhang DJ, Zhang YM, Liu CB (2006) J Phys Chem B 110:18267–18271
15. Korestune T, Saito S (2008) Phys Rev B 77:165417
16. Shan B, Cho K (2010) Chem Phys Lett 492:131–136
17. Zhang ZY, Cho K (2007) Phys Rev B 75:075420
18. Gong K, Du F, Xia Z, Durstock M, Dai L (2009) Science 323:760–764
19. Qu L, Liu Y, Baek JB, Dai L (2010) ACS Nano 4:1321–1326
20. Baierle RJ, Fagan SB, Mota R, da Silva AJR, Fazzio A (2001) Phys Rev B 64:085413
21. Avramov PV, Sorokin PB, Fedorov AS, Fedorov DG, Maeda Y (2006) Phys Rev B 74:245417
22. Galano A, Orgaz E (2008) Phys Rev B 77:045111
23. Guo GL, Wang F, Sun H, Zhang DJ (2008) Inter J Quant Chem 108:203–209
24. Jiang HH, Zhang DJ, Wang RX (2009) Nanotechnology 20:145501
25. Campos-Delgado J, Maciel IO, Cullen DA, Smith DJ, Jorio A, Pimenta MA, Terrones H, Terrones M (2010) ACS Nano 4:1696–1702
26. Fagan SB, Mota R, Baierle RJ, da Silva AJR, Fazzio A (2003) Mater Charact 50:183–187
27. Fagan SB, Mota R, da Silva AJR, Fazzio A (2004) Nano Lett 4:975–977
28. Zanella, Fagan SB, Mota R, Fazzio A (2007) Chem Phys Lett 439:348–353
29. Song C, Xia YY, Zhao MW, Liu XD, Li F, Huang BD, Zhang HY, Zhang BY (2006) Phys Lett A 358:166–170
30. Wang YW, Chen SG, Li L, Yin YS (2009) Multi-Funct Mater Struct 79:613
31. Mavrandonakis A, Froudakis GE (2003) Nano Lett 3:1481–1484
32. Perdew JP, Burke K, Ernzerhof M (1996) Phys Rev Lett 77:3865–3868
33. Delley B (1990) J Chem Phys 92:508–517
34. Delley B (2000) J Chem Phys 113:7756–7764
35. Monkhorst HJ, Pack JD (1976) Phys Rev B 13:5188–5192
36. Henkelman G, Jonsson H (2000) J Chem Phys 113:9978–9985
37. Olsen RA, Kroes GJ, Henkelman G, Arnaldsson A, Jonsson H (2004) J Chem Phys 121:9776–9792
38. Maciel IO, Campos-Delgado J, Cruz-Silva E, Pimenta MA, Sumpter BG, Meunier V, López-Urías F, Muñoz S, Oval E, Terrones H, Terrones M, Jorio A (2009) Nano Lett 9:2267–2272
39. Xu Z, Lu W, Wang W, Gu C, Liu K, Bai X, Wang E, Dai H (2008) Adv Mater 20:3615–3619
40. Li YT, Chen TC (2009) Nanotechnology 20:375705
41. Dean JA (1992) Lange's Chemistry H, book, 15th edn. McGraw-Hill, New York
42. Nakajima Y, Kameo H, Uzuki HS (2006) Angew Chem Int Ed 45:950–952
43. Dagani R (2007) Chem Eng News 85:67
44. Blum O, Milstein D (2002) J Am Chem Soc 124:11456–11467
45. Zhao J, Goldman JS, Hartwig JF (2005) Science 307:1080–1082
46. Lavallo V, Frey GD, Schoeller W, Bert G (2008) Angew Chem Int Ed 47:5224–5231
47. Ochi N, Nakao Y, Sato H, Sakaki S (2007) J Am Chem Soc 129:8615–8624
48. Frey GD, Lavallo V, Donnadieu B, Schoeller W, Bert G (2007) Science 316:439–441